

# RSC Advances



This is an *Accepted Manuscript*, which has been through the Royal Society of Chemistry peer review process and has been accepted for publication.

*Accepted Manuscripts* are published online shortly after acceptance, before technical editing, formatting and proof reading. Using this free service, authors can make their results available to the community, in citable form, before we publish the edited article. This *Accepted Manuscript* will be replaced by the edited, formatted and paginated article as soon as this is available.

You can find more information about *Accepted Manuscripts* in the [Information for Authors](#).

Please note that technical editing may introduce minor changes to the text and/or graphics, which may alter content. The journal's standard [Terms & Conditions](#) and the [Ethical guidelines](#) still apply. In no event shall the Royal Society of Chemistry be held responsible for any errors or omissions in this *Accepted Manuscript* or any consequences arising from the use of any information it contains.

# **Keloid collagen-cell interactions: Structural and functional perspective**

**Krishnaswamy Venkat Raghavan, Rachita Lakra and Korrapati Purna Sai\***

<sup>a</sup>Biomaterials Department

CSIR - Central Leather Research Institute,

Chennai, India – 600 020.

\* Corresponding Author: **Korrapati Purna Sai**

Email: [purusaik.clri@gmail.com](mailto:purusaik.clri@gmail.com) Telephone: 91-44-24437263, 91-44-24453491

## Abstract

Keloids are benign dermal proliferative disorder characterized by dense fibrotic tissue developing due to abnormal wound healing. Clinically, keloids extend beyond the margin of the original wound, do not undergo spontaneous regression and also recur after excision. Biochemical and cellular composition of keloids largely differ from that of normal dermis and mature scar plaguing physicians and patients for several decades. Keloids are rich in densely packed fibrillar collagen paralleled by up regulation of fibrogenic cytokines and growth factors. Adhesion of cells to the extracellular matrix (ECM) is a fundamental process during the formation and maintenance of animal tissue and therefore, aberrant cell-ECM interactions results in a number of diseases. There are numerous reports on the signaling mechanisms responsible for excessive production of collagen in the keloids. However, the structure-function correlation of collagen fibres in keloid is not understood properly. This paper is the first report to understand the influence of keloid collagen on the behaviour of fibroblasts with reference to cell adhesion, spreading and growth that translates the adhesion mediated signaling response in keloid pathogenesis. Cells grown on the normal collagen were well spread, adhered and proliferated while that on keloid collagen exhibited weak cell-matrix interactions and hence exhibited a lesser degree of proliferation. The differences observed in the cell behaviour could be attributed to the altered structural and thermal properties of the keloid collagen.

## Introduction

Keloids are human specific fibrotic lesions arising either spontaneously or during healing of deep dermal wounds. They are generally considered as benign tumours that are nodular in shape and extend beyond the clinical borders of the original wound. These lesions are therefore, characterized by lack of elastic fibres, abnormal collagen metabolism and elevated ECM constituents. Amongst the various parameters studied during keloid pathogenesis the epithelial - mesenchymal interactions generally involved in skin homeostasis have been found to significantly influence the fibroblast behaviour.<sup>1</sup> ECM has a significant role in the cell adhesion and maintenance of animal tissue integrity and morphology. Cellular interactions within the ECM are significantly complex and of central importance in various processes such as embryogenesis, differentiation and wound healing.<sup>2</sup> Collagen, the main constituent of ECM is not only essential for the mechanical resistance and resilience of tissues in the multicellular organisms but also serve as signaling molecule defining cellular shape and behaviour.<sup>3</sup>

Further, any aberrant communication between cells and their surrounding ECM is known to lead to a plethora of diseases like arthritis, fibrosis and cancer. Although extensive work has been carried out biochemically to understand the pathophysiology of keloid scarring<sup>4, 5</sup> there is a huge lacuna providing quantitative information about cell-substrate interactions in real time. Literature abounds in the ultra-structural morphology of keloid collagen depicting defective fibre orientation and organization.<sup>6</sup> However, a structural and functional perspective of keloid collagen with reference to cell-cell and cell-matrix

communication leading to an array of cellular responses such as adhesion, spreading and proliferation remains unearthed.

The electric cell-substrate impedance sensing (ECIS) model has emerged as a promising tool for quantitative determination of biochemical and physiological behaviour of cultured cells. ECIS measurements have been extensively used to characterize the anchorage dependent cell lines by Giaever and Keese.<sup>7</sup> This system has been designed to measure cell attachment, spreading<sup>8</sup>, motility<sup>9</sup> and also cell substrate interactions<sup>10</sup>. The device monitors the impedance of the cell-covered electrode using a lock in amplifier that returns both magnitude and phase of the voltage as a function of time.

In this study, we examined the morphological and growth behaviour of NIH 3T3 fibroblast cells on the collagen isolated from normal and abnormal scar tissues by comparing the calculated impedance values measured by ECIS using two adjustable independent parameters namely  $R_b$  and  $\alpha$ .  $R_b$  refers to the resistivity of the cell layer and  $\alpha = r_c (\rho/h)^{1/2}$  to the resistivity of the substratum beneath the cells, wherein  $r_c$  is the effective radius of the spread cell and  $\rho$  is the resistivity of the solution and  $h$  is the average distance between the cells and the substratum.<sup>11</sup> This report therefore, is the first attempt to understand the possible influence of the keloid collagen on cell adhesion, spreading and growth which could probably account for the abnormal cell signaling mechanism involved in keloid formation.

## Materials and Methods

### Collagen Extraction

Keloid, hypertrophic scar and normal skin biopsies were collected during cosmetic surgery after prior consent from the patients and in compliance with ethical guidelines of CSIR-Central Leather Research Institute, Chennai and Kilpauk Medical College Hospital, Chennai, India. The age of Keloid and hypertrophic scar tissue was 1 year and 10 months respectively. All the tissue samples extensively washed with phosphate buffered saline (PBS) were immediately used for collagen extractions as described by Sai and Babu.<sup>12</sup> All the studies involved pepsin-treated collagen and the concentration of collagen was determined by its hydroxyproline content as described by Woessner.<sup>13</sup> The collagens extracted was either immediately used or stored as lyophilized form at - 20<sup>0</sup> C.

### Gel Electrophoresis

SDS PAGE was performed according to the procedure of Laemmli.<sup>14</sup> Collagen samples were mixed with loading buffer (Tris-HCl, glycerol,  $\beta$  - mercaptoethanol and bromophenol blue) in 1:1 ratio to reach a final collagen concentration of 10  $\mu$ g. The samples were denatured in boiling water bath for 2 min. and subjected to electrophoresis in a 3 % stacking and 6 % resolving gel using a Mini Protean electrophoresis unit (Bio – Rad). The gel was then stained with 0.25% Coomassie brilliant blue R-250 (Sigma-Aldrich) for 60 min. and destained with a solution of 10% glacial acetic acid, 25% methanol, and 65% water until the bands were clear.

### **Fourier Transform Infrared Spectroscopy**

The collagen extracted from keloid, hypertrophic scar and normal skin tissue samples were mixed with approximately five times of vacuum dried potassium bromide and pressed into pellets which were characterized using Fourier Transform infrared spectroscopy (FTIR). (Model No. MB 300-PH, ABB).

### **Thermogravimetric Analysis**

The thermogravimetric analysis was performed in a nitrogen atmosphere using thermogravimetric analyser (Model No. Q50 V 20.6, TA Instruments). The scanning was performed up to 800°C at a heating rate of 20°C / min.

### **Differential Scanning Calorimetry**

The denaturation temperature of the collagens was determined by a differential scanning calorimetry apparatus (Model No. Q200 V23.10, TA Instruments). The samples were hermetically sealed in aluminium pans and heated at a constant rate of 10<sup>0</sup> C / min. The endothermal curves of the samples were recorded from 25-300<sup>0</sup> C in an inert nitrogen atmosphere.

### **Collagen reconstitution and coating**

Collagen (1 mL of 0.5 mg / mL) was mixed with 100 µL of phosphate buffer (0.2 M) and 75 µL of sodium chloride (2 M) and the reconstitution was initiated by adjusting the pH to 7.2 using sodium hydroxide (1.25 N). The solution was then coated onto the culture dish and allowed to form gel by incubating at 37° C. The gels were then allowed to dry and washed extensively with PBS (pH 7.2) to remove the adhered salts. The plates were sterilized by UV radiation prior to seeding NIH 3T3 cells.

### **Cell culture studies**

The mouse fibroblast cell line NIH 3T3, was obtained from National Centre for Cell Science, Pune, India. The cells were cultured in Dulbecco's Modified Eagle Medium (DMEM, D1152, Sigma-Aldrich) supplemented with 10 % foetal bovine serum, sodium bicarbonate (3.7 mg / mL), streptomycin (100 µg / mL), penicillin (100 units / mL), gentamicin (30 µg / mL) and fungizone (2.5 µg / mL). The cells were maintained at 37°C in a humidified 5 % CO<sub>2</sub> incubator (CB150, Binder) in 25 cm<sup>2</sup> flasks. All chemicals were cell culture tested and procured from Sigma-Aldrich.

### **Cell proliferation assay**

The proliferative potential of NIH 3T3 fibroblast cells on collagen isolated from keloid, hypertrophic scar and normal skin was assessed by MTT (3-(4, 5-Dimethylthiazol-2-yl)-2, 5-diphenyltetrazolium bromide) assay.<sup>15</sup> Uniform number of cells was seeded onto a culture dish coated with different collagens and allowed to proliferate for 48 and 72 hours. The growth as an index of cell proliferation was measured spectrophotometrically (Lambda 45, UV / Vis Spectrometer, Perkin Elmer.) at 570 nm after treating with MTT for 3 hours.

### **Cell behaviour on the gold electrode (ECIS)**

Electrode array (8W1E, Applied Biophysics Inc.) with eight wells containing a 250 µm diameter gold electrode ( $5 \times 10^{-4}$  cm<sup>2</sup>) and a larger gold counter electrode (0.15 cm<sup>2</sup>) were stabilized by incubating with DMEM (without serum and antibiotics) for one hour at 37°C. The collagen obtained from keloid, hypertrophic scar and normal skin was



reconstituted as described earlier and coated in duplicate on to the array wells. The wells were washed with PBS, sterilized by UV radiation and used for the experiments.

Uniform number of  $1 \times 10^5$  cells / well were seeded on an ECIS array (8W1E) and incubated at  $37^\circ \text{C}$ . The attachment and spreading of the cells on the collagen substrata were analyzed by impedance measurements at 6000 Hz. In addition to the total impedance measurements, resistance and capacitance were also determined considering the cell electrode system as a series RC circuit.

### **Cell adhesion assay**

The collagens were reconstituted as described earlier and coated onto a 96 well tissue culture plate. NIH 3T3 cells were inoculated at a density of  $3 \times 10^4$  cells / well and were incubated for 4 hours at  $37^\circ \text{C}$ . After incubation the wells were washed gently with warm PBS for 3-5 times to remove the non-adherent cells. The cells were then fixed with 96 % ethanol for 10 min and stained with 0.1 % crystal violet for 30 min. Excess dye was removed by washing the wells thoroughly with deionized water. The absorbed dye was then extracted using acetic acid and the absorbance was measured at 570 nm in a microplate reader (Bio-Rad.)

### **Scanning Electron Microscopic study**

Uniform number of cells grown keloid and normal collagen coated Thermanox® cover slips were fixed with 2 % glutaraldehyde. The cells were again re-fixed with 1 % osmium tetroxide after washing thrice with 0.1 M sodium cacodylate buffer. The samples were then dehydrated with increasing gradients of water-acetone mixtures followed by treatment with increasing gradients of acetone-hexamethyldisilazane mixtures. The

samples were snap frozen with liquid nitrogen and freeze dried in a lyophilizer. The samples were then gold sputter coated under argon atmosphere and viewed under high vacuum using a scanning electron microscope (SEM) (Hitachi).

### **Statistical Analysis**

All experiments were repeated thrice. Data shown are the mean of the three repeated results.

### **Results**

#### **Electrophoretic Mobility**

The electrophoretic patterns of the collagens were shown in the Fig. 1A. All collagens displayed alpha, beta and gamma components. The  $\alpha_1:\alpha_2$  band ratio was more than 2:1 depicting that all the samples contain more than one type of collagen. The  $\beta$  and  $\gamma$  components an indication of presence of cross-linked collagen was found to be high in keloids when compared to normal sample.

#### **Structural Characterization**

The FTIR spectra of collagen from keloid, hypertrophic scar and normal (Fig.1B) showed the presence of amide A band at  $3424\text{ cm}^{-1}$ ,  $3324\text{ cm}^{-1}$  and  $3420\text{ cm}^{-1}$  respectively indicative of the free NH stretching frequency.<sup>16</sup> The free NH stretching frequency in the keloid collagen was slightly higher than that of normal and hypertrophic scar. This could be probably due to the increased hydrogen bonding or water mediated hydrogen bonding. This was also be confirmed from the DSC experiments, where the initial temperature required for water loss is higher in keloid collagen than normal and hypertrophic scar

(Fig. 2A) suggesting that a lesser water mediated hydrogen bonding exist in normal collagen when compared to keloid collagen. Thus, the enhanced cross linking in the keloid collagen samples could therefore be more through the water mediated hydrogen bonding and hence probably less stable than the normal collagen. All the three collagen samples showed a characteristic collagen band at  $1655\text{ cm}^{-1}$ <sup>17</sup> and amide II band around  $1550\text{ cm}^{-1}$ .<sup>18</sup> The triple helical nature of all the three collagens were confirmed by the ratio between the peaks observed at  $1450\text{ cm}^{-1}$  and  $1238\text{ cm}^{-1}$  (amide III) which approximately equals to one.<sup>19</sup>

### Thermal Analysis

The thermograms of all the three collagens depicted in Fig. 2A correlated with the shrinkage temperature of dry fibrous collagen. The collagen extracted from keloid, hypertrophic scar and normal skin biopsies when heated up to  $50^\circ\text{C}$  did not show any significant changes in their thermodynamic properties indicating that the collagen was intact. Further heating induced a transition from collagen to gelatin, which at molecular level involves the conversion of rigid three-chain collagen molecule to random coil gelatin. The shift in the denaturation temperature with reference to keloid could be attributed to the thick and short triple helical moieties in comparison to long narrow fibrils in normal collagen.

The degradation of all collagens (Fig. 2B) was initiated at  $200\text{-}230^\circ\text{C}$ , the typical protein polypeptide thermal degradation temperature.<sup>20</sup> The final heating phase  $600\text{-}750^\circ\text{C}$  related to the combustion of residual organic matter was rapid for keloid collagen than that of normal and hypertrophic scar. The results suggested that although the initial denaturation temperature in keloid collagen required slightly higher temperature, the

stability is lesser than that of hypertrophic scar and normal skin. This could be attributed to the differences in the nature and the arrangement of the collagen fibrils.

### **Cell proliferation analysis**

The fibroblasts exhibited increased proliferation and growth potential as observed by MTT assay on the normal skin collagen in comparison to the collagen isolated from the abnormal scars. (Fig. 3A) The growth curve trend of fibroblasts may be depicted as growth on normal skin collagen > hypertrophic scar collagen > keloid collagen. Therefore, the growth studies on the various collagen substrata suggested that the cell-cell interaction as well as cell - matrix interaction play a crucial role in determining the cell growth potential.

### **Adhesion analysis**

The cell adhesion assay indicated that NIH 3T3 cells adhered well to normal collagen than hypertrophic scar and keloid collagen (Fig. 3B). The results showed that the cell matrix interaction was weak on the keloid collagen as substantiated by the alpha values on the ECIS system.

### **Cell substrate interactions on gold electrode**

The electric cell impedance measurements indicated that the resistance (Fig. 4A) to the flow of current exhibited by the cells was profound when normal skin collagen was used as substratum in comparison to that of hypertrophic scar and keloid collagen. This behaviour correlated perfectly with the results of the MTT assay. The extent of closest contact between basal membrane of the cells and the substratum is less before cell adhesion and increases continuously until the cells assume their characteristic shape. The cell membrane being an insulator restricted the current flow forcing it to flow only

through the narrow channels underneath the cells before escaping into the bulk electrolyte at the cell perimeter.<sup>10</sup> The pictorial representation of  $R_b$  and  $\alpha$  has been detailed in Scheme.1 (<http://www.biophysics.com/>). The  $R_b$  and  $\alpha$  were calculated based on the model described by Giaever and Keese.<sup>9</sup> The  $R_b$  function across the collagen - coated electrodes and the impedance measured in terms of  $\alpha$  is indicated in the Fig. 4B. The  $R_b$  was high for the cells grown on normal collagen followed by hypertrophic scar and then by keloid collagen. The measurement of  $\alpha$  is more prominent than the  $R_b$  suggesting the significance of the substrata. In this model, the cells are described as circular disks of radius  $r_c$  that are spaced on average distance  $h$  above the substrate.

The impedance of the cell covered electrode was then dependent on the impedance of the electrode itself, the resistance between adjacent cells  $R_b$ , the capacitance of the cell membrane  $C_m$ , and a parameter  $\alpha = r_c \cdot (\rho/h)^{1/2}$ . This depends on the average distance between basal plasma membrane and the substrate  $h$ . The  $R_b$  function measurements indicated the resistance barrier for the current flow through the narrow spaces between the cells<sup>21</sup> which suggested that tight junctions established between the cells. Thereby, the  $R_b$  fluctuation with reference to keloid being not very significant indicated that the cell-cell interactions were not much affected by the substrata. On the other hand, the reduced  $\alpha$  value for keloid substratum unlike normal and hypertrophic substrata indicated that the cell substrate interactions were significantly weak.

### **Morphological analysis**

The behaviour of NIH 3T3 grown on normal and keloid collagen substrata were compared by SEM (Fig. 4C). The results showed that unlike keloid collagen the cells adhered and spread well on the normal collagen. Moreover, the cells on the normal

collagen were evenly distributed whereas the cells on the keloid collagen were closely packed indicating that the fibril structure of collagen was important for cell behaviour.

## Discussion

Collagen fibril alignment was vital for the attachment of cells suggesting that orientation and thickening of the collagen fibrils characteristic of keloid skin prevented the tight attachment of the cells. A higher  $R_b$  indicated significant interactions amongst the cells while a high  $\alpha$  measurement was the representative of the constricted current flow beneath the cells. Therefore, the high  $\alpha$  value was a direct measure of cell attachment to substrate. These measurements suggested that cell attachment on the keloid collagen substrata was significantly weak in comparison to the normal and hypertrophic scar collagen. This might be attributed to the reduced growth potential of cells on the keloid collagen substrata.

Binding interactions between cells and surfaces are influenced by spatial domains, structural compositions and mechanical forces at micro and nanoscale level.<sup>22</sup> Majority of the previous studies indicated that the collagen bundle orientation parallel to the epithelial surface was characteristic of hypertrophic scars and keloids while a basket weave network pattern characterized normal skin.<sup>23</sup> Further, the bundle distribution was more random and haphazard in keloids in comparison to the other scars.<sup>24, 25</sup> Despite the absence of basic structural differences amongst the collagen extracted from the various tissues, the behaviour of the cells was significantly different. This may be attributed to the fibril length, thickness, orientation and composition thereby altering the cell matrix interactions. A cell proliferation or death does not depend on the amount of integrin-ligand binding but by the degree to which a cell physically extends.<sup>22</sup>

Although novel strategies emerged for visualizing the structure and interactions inside the cells, the insulating cell membrane limits the monitoring of functions of most proteins and tracking of the plethora of protein-protein interactions.<sup>22</sup> Cellular activity in reality is defined by a network of interactions involving protein conformation changes; membrane bound protein signaling, ion gradients and active transport along the cytoskeleton. Understanding the adhesion mediated response of cells is highly dependent on the composition and the characterization of the underlying substrate. The cells when tightly confined to each other tend to perform tissue specific functions. On the other hand proper adherence of cells to the matrix is essential for its proliferation.<sup>26,27</sup> Thus, the cells on normal and hypertrophic scar collagen were well adhered and hence, exhibited increased proliferation while that on keloid collagen were less adhered attributing to restricted proliferation. This may also be due to the increased ligand density clustering and enhanced adhesive signaling because cell - substrate interactions are involved in eliciting the focal adhesion, intracellular signaling, propagation of cell spreading and integrin clustering.

Hence, the alignment and orientation of the fibrils influence the surface chemistry and microstructures of the collagen, which in turn facilitate cellular attachment, proliferation and differentiation crucial for tissue regeneration

## **Conclusions**

This study therefore, envisages the importance of the collagen architecture with reference to the bundle thickness, orientation and composition of the individual fibrils responsible for the objective differences in cell behaviour on the different substrata. In conclusion,

keloid pathogenesis is thereby influenced not only by the abnormal collagen metabolism but also due to the behavioural aspects translated through adhesion mediated response.

### **Acknowledgements**

The authors thank Prof. Dr. A. B. Mandal, Director CSIR- Central Leather Research Institute for his encouragement and support. The authors also acknowledge the help of Dr. V. Jayaraman, Kilpauk medical college, Chennai in harvesting the tissue samples. This work was financially supported and the ECIS system was procured from the funds of the project (No.BT/PR8148/GBD/27/22/2006) sanctioned by Department of Biotechnology, (DBT) Government of India.



## References

1. A. M. Pizzo, K. Kokini, L.C. Vaughn, B. Z. Waisner and S.L. Voytik-Harbin, *J. Appl. Physiol.*, 2005, 98,1909.
2. W. P. Daley, S. B. Peters and M. Larsen, *J. Cell.Sci.*, 2008, 121, 255.
3. W. F. Vogel, *Eur. J. Dermatol.*, 2001, 11, 506.
4. T. T.Phan, I. J. Lim, O. Aalami, F. Lorget, A. Khoo, E. K. Tan, A. Mukhopadhyay and M. T. Longaker, *J. Pathol.*, 2005, 207, 232.
5. G. M. Bran, U. R. Goessler, K. Hormann, F. Riedel and H. Sadick, *Int. J. Mol. Med.*, 2009, 24, 283.
6. V. Prathiba, R. Kumaresan, M. Babu and P. D. Gupta, *Biomed.Lett.*, 1998, 58, 41.
7. I. Giaever and C. R. Keese, *Proc. Natl. Acad. Sci.*, 1984, 81, 3761.
8. P. Mitra, C. R. Keese and I. Giaever, *BioTechniques.*, 1991, 11, 504 .
9. I. Giaever and C. R. Keese, *Proc. Natl. Acad. Sci.* 1991, 88, 7896.
10. J. Wegener, C. R. Keese and I. Giaever, *Exp. Cell. Res.*, 2000, 259, 158.
11. C. M. Lo, C. R. Keese and I. Giaever, *Biophy.J.*, 1995, 69, 2800.
12. K. P. Sai and M. Babu, *Comp. Biochem.Physiol. – Part B.*, 2001, 128, 81.
13. J. F. Jr. Woessner, *Arch. Biochem.Biophys.*, 1961, 93, 440.
14. U. Laemmli, *Nature*, 1970, 227, 680.

15. T. Mosmann, *J. Immunol.Meth.*, 1983, 55, 55.
16. M. Zhang, W. Liu and G. Li, *Food Chem.*, 2009, 115, 826.
17. D. A. Prystupa, A. M. Donald, *Polymer Gels and Networks*, 1996, 4, 87.
18. B. D. C. Vidal and M. L. S. Mello, *Micron*, 2011, 42, 283.
19. A. M. de GuzziPlepis, G. Goissis and D. K. Das-Gupta, *Polymer Engineering & Science.*, 1996, 36, 2932.
20. Y. Di and R. J. Heath, *Polym.Degrad. Stab.*, 2009, 94, 16842.
21. L. Treeratanapiboon, K. Psathaki, J. Wegener, S. Looareesuwan, H. J. Galla and R. Udomsangpetch, *Biochem. Biophys. Res. Commun.*, 2005, 335, 810.
22. N. J. Sniadecki, R. A. Desai, S. A. Ruiz and C. S. Chen, *Ann. Biomed. Eng.*, 2006, 34, 59.
23. P. D. Verhaegen, P. P. van Zuijlen, N. M. Pennings, J. Van Marle, F. B. Niessen and C.M.van der Horst and E. Middelkoop, *Wound Repair Regen.*, 2009, 17, 649.
24. T. R. Knapp, R. J. Daniels, and E. N. Kaplan, *Am. J. Pathol.*, 1977, 86, 47.
25. J. Y. Lee, C. C. Yang, S. C. Chao and T. W. Wong, *Am. J. Dermatopathol.*, 2004, 26, 379.
26. C. S. Chen, M. Mrksich, S. Huang, G. M. Whitesides and D. E. Ingber, *Science*, 1997, 276, 1425.

27. R. Singhvi, A. Kumar, G. P. Lopez, G. N. Stephanopoulos, D. I. Wang, G. M. Whitesides and D. E. Ingber, *Science*, 1994, 264, 696.

## Figure Legends

*Fig. 1A: Electrophoretic pattern of collagen isolated from Keloid (K), Hypertrophic Scar (H) and Normal (N).*

*1B: Infrared spectra of pepsin-treated collagen extracted from (a) Keloid (b) Hypertrophic scar and (c) Normal skin biopsies.*

*Fig 2A: Differential scanning calorimetric scans of collagen isolated (a) Keloid (b) Hypertrophic scar (c) Normal skin biopsies.*

*2B: Thermogravimetric analysis of collagen extracted from (a) Keloid (b) Hypertrophic scar (c) Normal skin biopsies.*

*Fig.3A: Growth potential of NIH 3T3 fibroblast on reconstituted collagen.*

*3B: Adhesion potential of NIH 3T3 fibroblasts on Normal, Hypertrophic scar and Keloid collagen*

*Fig.4A: Cell behaviour on the collagen isolated from Normal (N), Hypertrophic scar (Hs) and Keloid (K) measured using electric cell impedance system (ECIS) at 6000 Hz.*

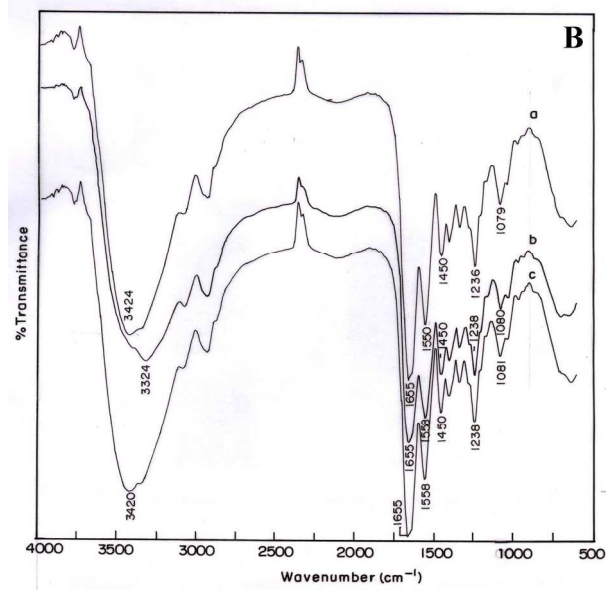
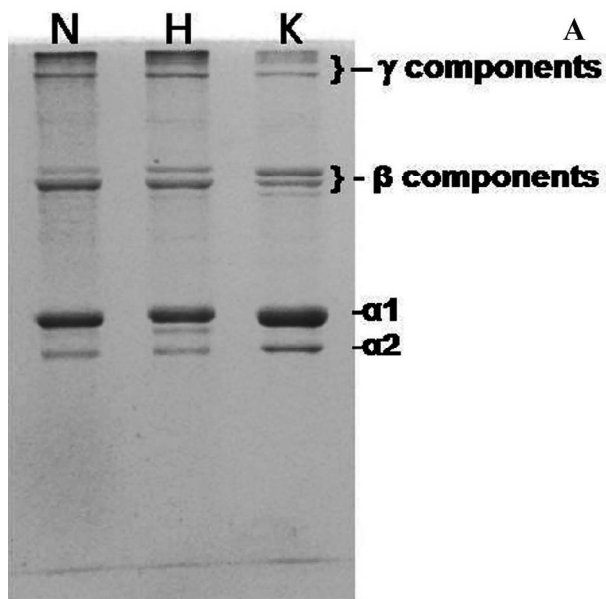
*4B: (a) Barrier function ( $R_b$ ) (b) alpha ( $\alpha$ ) measured using ECIS system at 6000 Hz on the different collagen substrata.*

*4C: Scanning electron micrographs of NIH 3T3 fibroblasts on a) Normal collagen b) Keloid collagen*

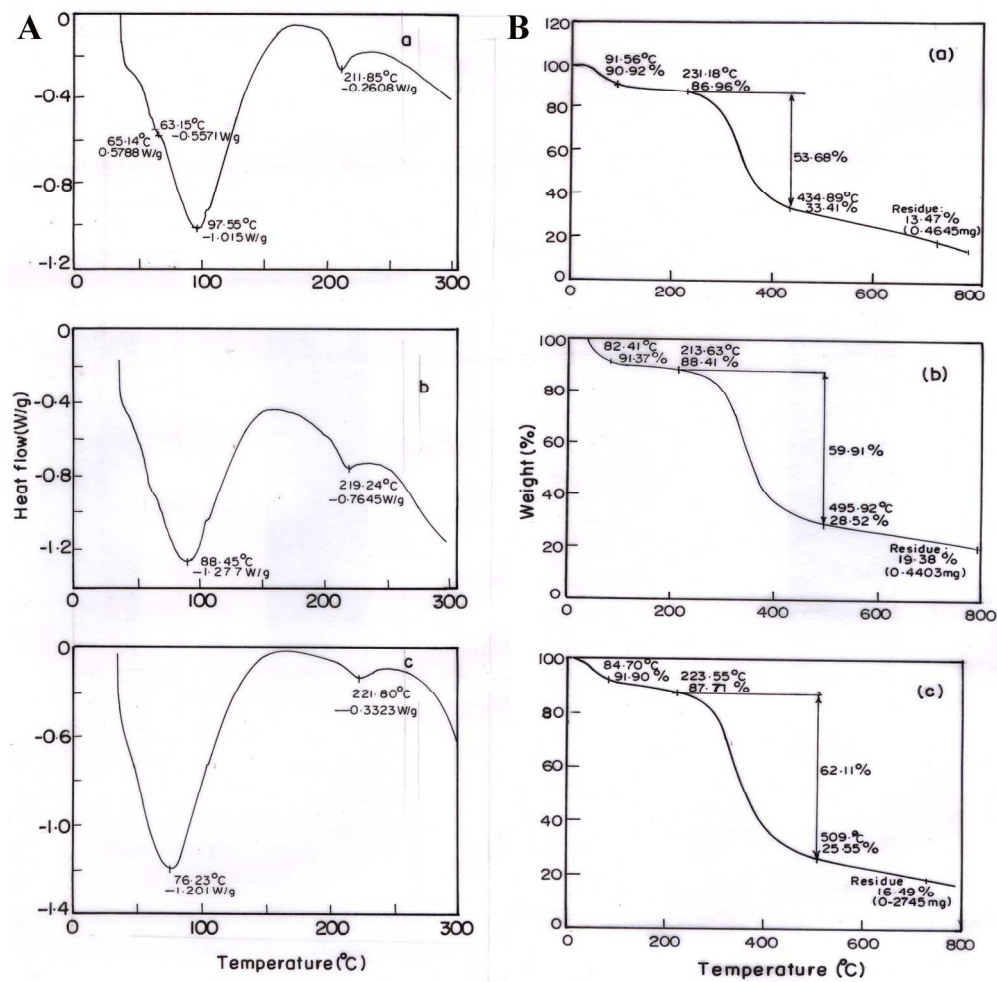
*Scheme 1: Pictorial representation of cell interaction with substratum on the electrode with reference to barrier function ( $R_b$  and alpha ' $\alpha$ ').*





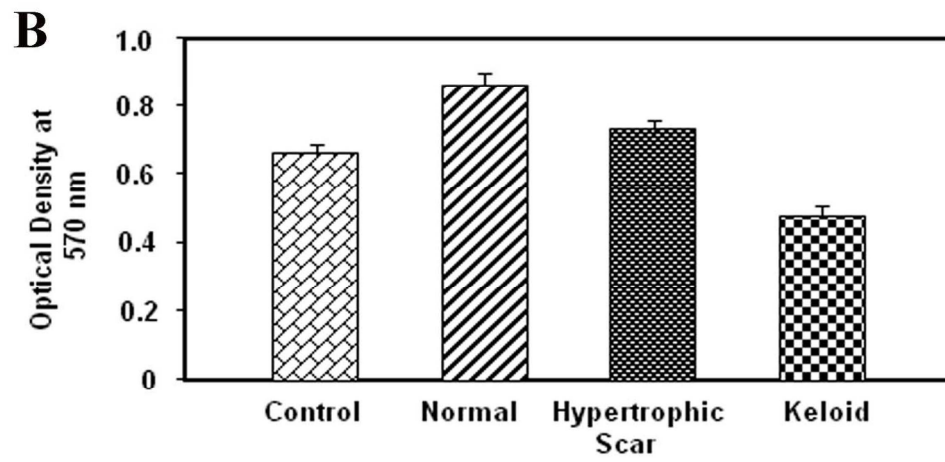
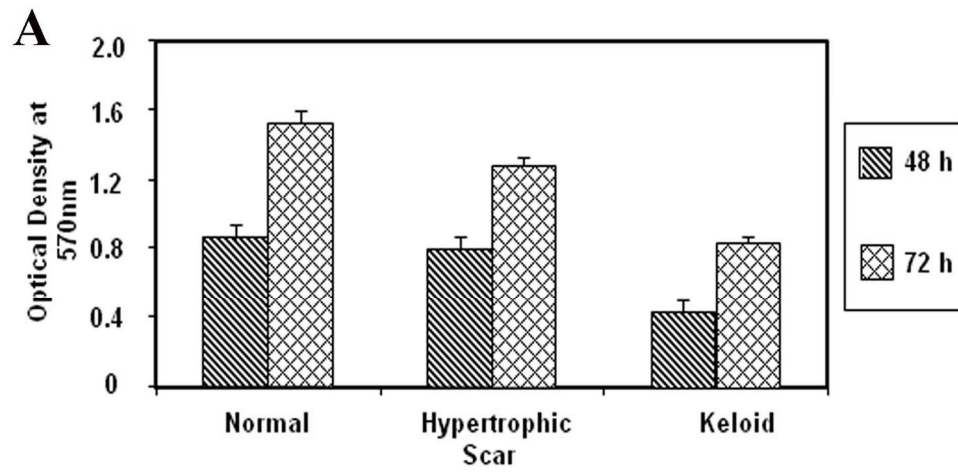


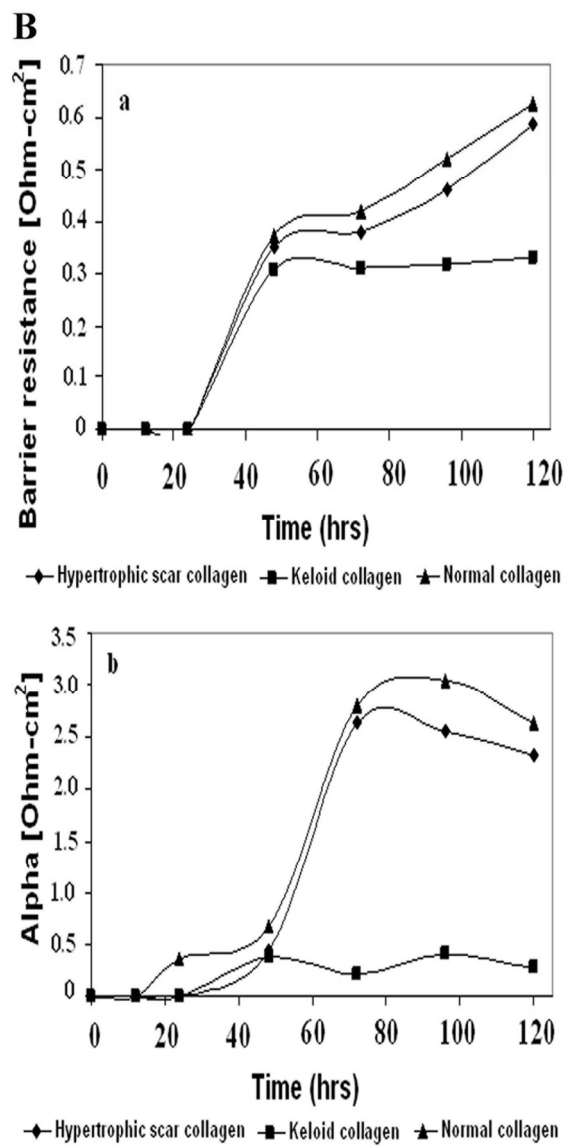
199x399mm (300 x 300 DPI)

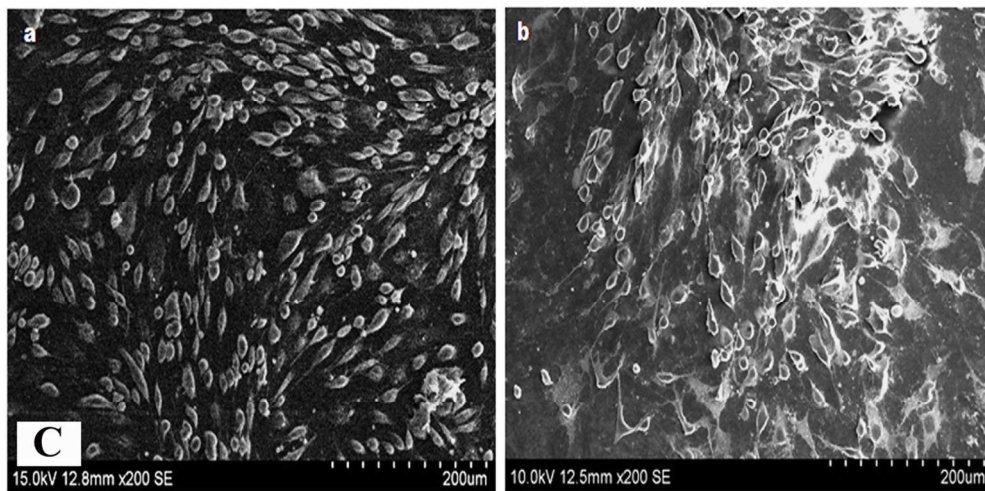


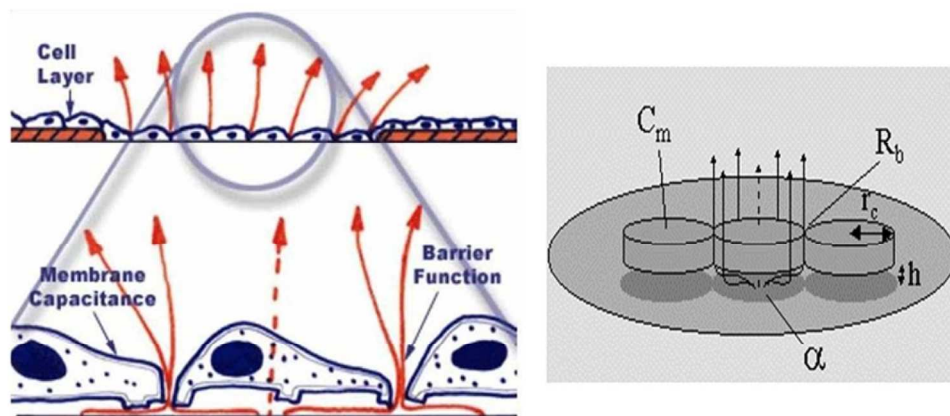
299x299mm (300 x 300 DPI)



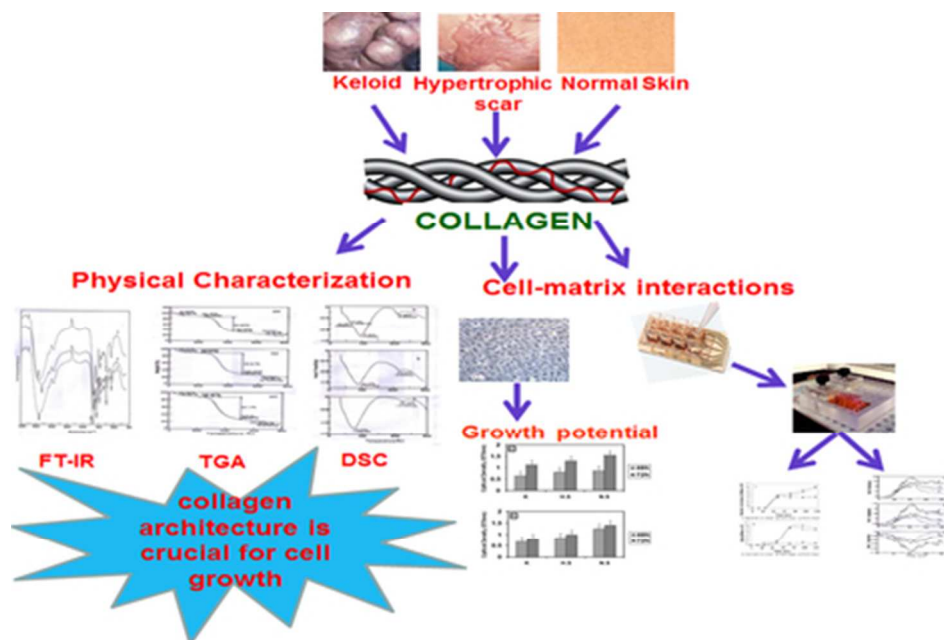








210x127mm (300 x 300 DPI)



39x26mm (300 x 300 DPI)